Publ. Astron. Soc. Japan 37, 439–450 (1985)

CO Observations of a Spiral Arm in M31*

Takashi ICHIKAWA, Makoto NAKANO, Yutaka D. TANAKA, and Mamoru SAITŌ

Department of Astronomy, University of Kyoto, Sakyo-ku, Kyoto 606

and

Naomasa NAKAI, Yoshiaki SOFUE, and Norio KAIFU

Nobeyama Radio Observatory, Minamimaki-mura, Minamisaku-gun, Nagano 384-13

(Received 1984 August 21; accepted 1985 February 14)

Abstract

Using the 45-m telescope of the Nobeyama Radio Observatory, we have carried out observations of ^{12}CO (J=1–0) line emission in the southern arm of M31, where the most conspicuous dark cloud and a complex of H II regions are located. The angular resolution of 14″ corresponds to a linear resolution of 47 pc at the distance of M31. The CO-arm width was found to be about 500 pc and the CO emitting region seems to avoid the H II regions. An average surface density of molecular hydrogen is $16M_{\odot}$ pc^{-2} in the CO arm as derived from the integrated CO emission. The CO emission consists of broad and narrow line features, for which the full widths at half intensity range from 3 to 23 km s^{-1}. The broad components with the full velocity width of ΔV=9–23 km s^{-1} are more or less spatially continuous and may be due to many small CO clouds with a cloud-to-cloud velocity dispersion similar to that in the solar neighborhood. The narrow components of ΔV=3–5 km s^{-1}, which look more patchy, are due to individual CO clouds with masses of about $(2\text{–}6)\times10^{4}M_{\odot}$. The mean radial velocities of the broad emission lines in the dense arm have systematic deviation of 9–18 km s^{-1} from those expected from a circular rotation. On the other hand, the velocities outside the dense arm are consistent with a circular rotation. This velocity discontinuity can be attributed to the deceleration by the spiral arm shock.

Key words: CO line emission; Galaxies; Interstellar molecules; M31; Spiral arms.

1. Introduction

Stark (1985) has presented a map of integrated ^{12}CO line emission (J=1–0) in a

* Based on observations made at the Nobeyama Radio Observatory (NRO). NRO, a branch of the Tokyo Astronomical Observatory, University of Tokyo, is a facility open for general use by researchers in the field of astronomy and astrophysics.

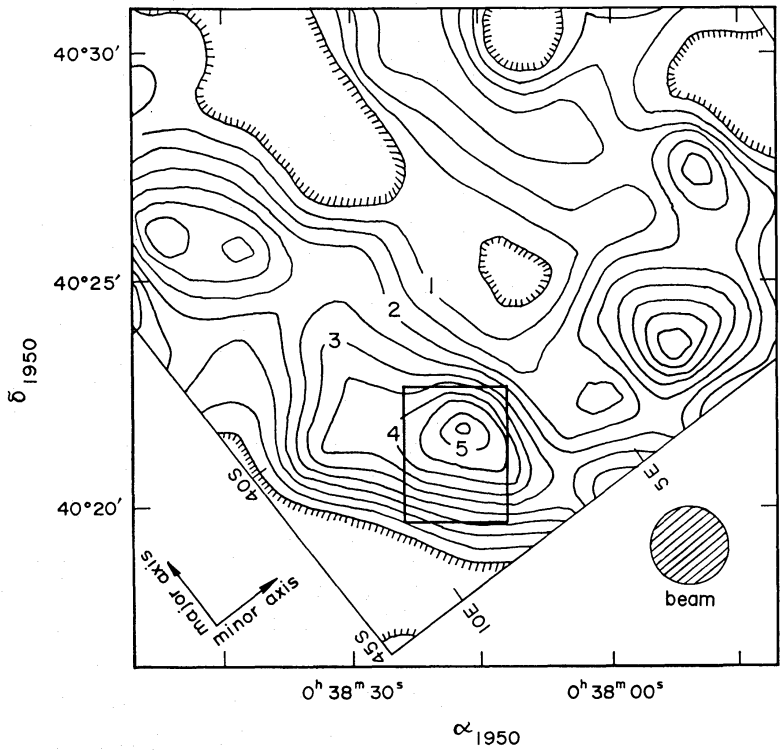

Fig. 1. The contour map of integrated ^{12}CO emission (K km s^{-1}) at the southern part of M31 (Stark 1985). It is sampled with 1′.7 beam at half power on a 1′.1 square grid. Our investigated region is shown with a box. Arrows indicate the directions of the major and minor axes of M31. The coordinates follow Brinks and Shane (1984).

15′×18′ field of the southern arm of M31 with a spatial resolution of 1′.7. His map shows several large cloudlike structures with sizes as large as several hundred parsecs to 1 kpc across. The largest cloud centered on $(\alpha_{1950}, \delta_{1950})=(0^h38^m17^s, 40°21'.7)$ is associated with the most conspicuous dark cloud and has an apparent size of 1 kpc ×500 pc at the 690 kpc distance of M31 (figure 1). Boulanger et al. (1981) have estimated its total H_2 and H I masses to be $M_{H_2}=3.14\times10^6 M_\odot$ and $M_{H\,I}=2.25\times10^7 M_\odot$.

A large molecular cloud complex in our Galaxy is, however, ∼100 pc in linear extent size and $\sim10^5 M_\odot$ in mass (Stark and Blitz 1978). Therefore such mass and apparent size of the much larger cloud in M31 lead us to the idea that it consists of many CO clouds forming a large cloud complex. The highest resolution so far attained in CO observations of M31 is 1′.1 (Combes et al. 1977; Blitz 1981), which corresponds to a size of 220 pc. This resolution is not high enough to detect individual CO clouds. In order to investigate the fine structure of the largest cloud, we have observed the ^{12}CO line emission with a spatial resolution of 14″, or 47 pc at the distance of M31.

2. Observations

The observations were carried out on March 5 through 7, 1984 with the 45-m telescope of the Nobeyama Radio Observatory (NRO). The half-power beam width

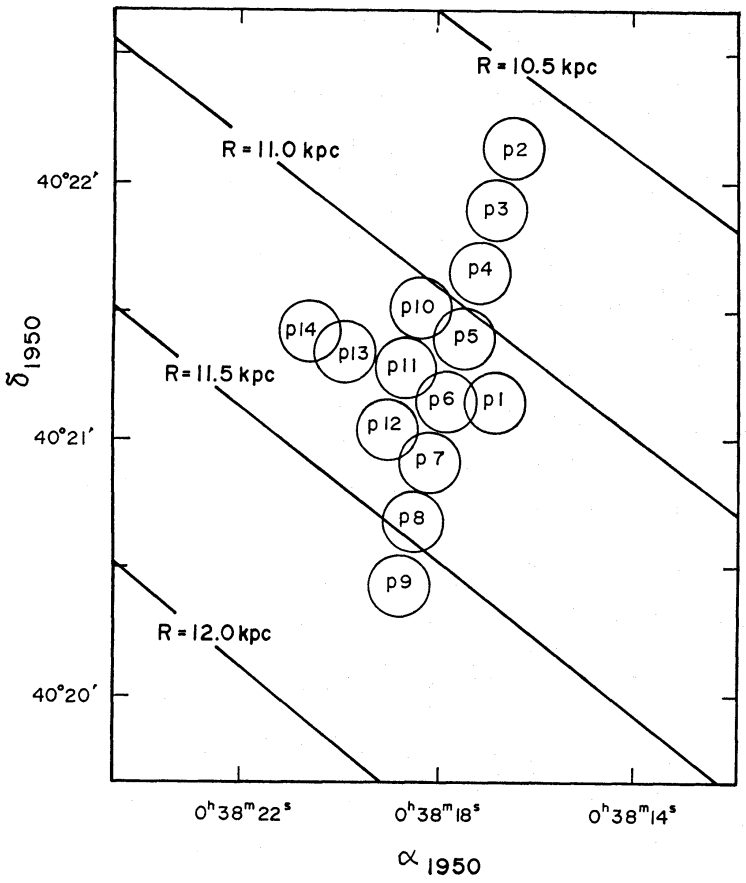

Fig. 2. Observed points. The circles represent the telescope beam of 14″ at half power, which corresponds to 47 pc in M31. Solid lines show equidistance R from the center of M31.

is 14″ at the observing frequency of 115 GHz. The observed points are shown in figure 1 with a box and in figure 2 with circles of 14″ in diameter.

We used a cooled receiver with a Schottky barrier diode mixer with a single-side band system noise temperature of about 800 K. The spectra presented in this paper were taken with a 2048-channel acoustooptical spectrometer. The frequency resolution is 250 KHz which corresponds to a velocity resolution of 0.65 km s^{-1}. The efficiency of the main beam and the aperture of the antenna at 115 GHz was about 0.3 and 0.25, respectively. The pointing accuracy was determined to be better than 10″ r.m.s. by frequently measuring the 43-GHz SiO maser line of R Cas ($\alpha_{1950}=23^{h}55^{m}52^{s}.0$, $\delta_{1950}=51°6'36''$).

The data were obtained by position switching every 30 s between the source and a reference position away from the disk of M31. Each map point was observed for about one hour. The temperature calibrations were made with an absorbing chopper at room temperature in front of the receiver to obtain antenna temperature, T_A^*, corrected for the atmospheric absorption and ohmic losses.

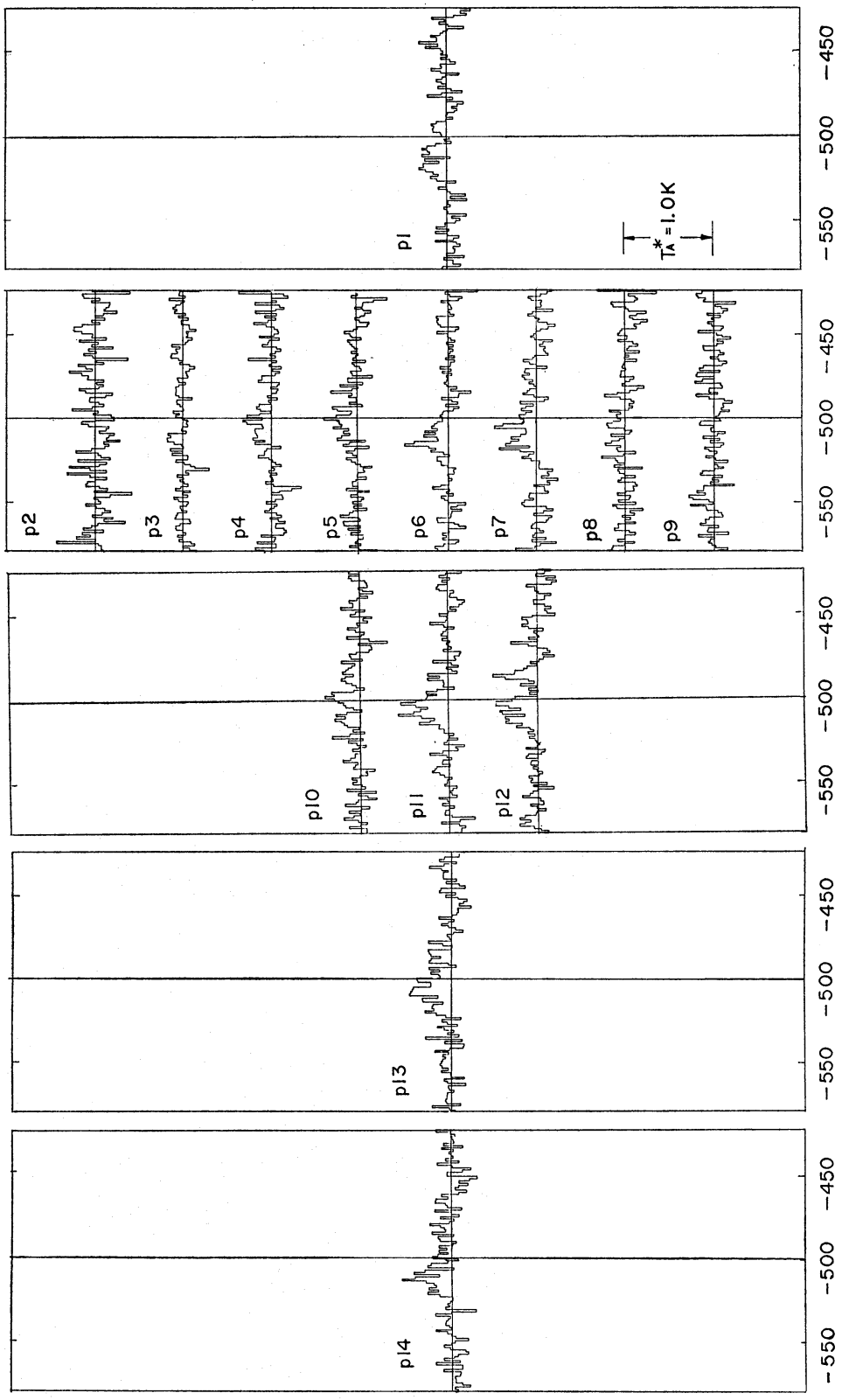

Fig. 3. The observed CO profiles for the points shown in figure 2. The velocity is heliocentric. The velocity resolution is reduced to 1.3 km s^{-1}.

3. Results

The observed spectra are displayed in figure 3, where the velocity resolution is reduced to 1.3 km s^{-1}. Table 1 lists the observational results. The positions are given by the offset values ($\Delta\alpha$, $\Delta\delta$) from P4 ($\alpha_{1950}=0^h38^m17^s.1$, $\delta_{1950}=40°21'39''$), which is the same position as M31-6 of Combes et al. (1977) or (−42.1, 7.7) of Boulanger et al. (1981). The third and fifth columns of table 1 list the peak antenna temperature and its velocity (heliocentric) for each observational point, respectively. The r.m.s. noises are given in the fourth column.

Table 1. Observational results.

Observed point	Position† ($\Delta\alpha$, $\Delta\delta$)	T_A* (K)	σ_{rms} (K)	V_{peak} (km s^{-1})
P 1	(− 5″, −30″)	0.32	0.07	−520
P 2	(−10 , 29)	...	0.12	...
P 3	(− 5 , 14)	...	0.07	...
P 4	(0 , 0)	0.31	0.11	−502
P 5	(5 , −15)	0.37	0.07	−501
P 6	(10 , −30)	0.49	0.06	−516
P 7	(15 , −44)	0.48	0.07	−506
P 8	(20 , −58)	...	0.09	...
P 9	(25 , −73)	...	0.12	...
P10	(18 , − 7)	0.40	0.07	−500
P11	(23 , −22)	0.57	0.07	−510
P12	(28 , −36)	0.53	0.07	−487
P13	(38 , −17)	0.48	0.12	−510
P14	(52 , −13)	0.57	0.08	−514

† Offset position from P4 ($\alpha_{1950}=0^h38^m17^s.1$, $\delta_{1950}=40°21'39''$).

Table 2. Quantities for the observed emission features.

Observed point	Velocity range (V_1, V_2) (km s^{-1})	$\langle V\rangle_{CO}$ (km s^{-1})	ΔV (km s^{-1})	$\langle V\rangle_{CO}-V_{rot}$ (km s^{-1})	$\int_{V_1}^{V_2} T_A^* dV$ (K km s^{-1})	N_{H_2}† (10^{20} cm^{-2})	σ_{H_2}† ($M_\odot$ pc^{-2})
P 1	(−526, −491)	−511	16	−15	10.8±0.5	8.7	14
P 4	(−516, −493)	−504	10	− 6	7.2±0.6	5.8	9
P 5	(−528, −477)	−501	16	− 5	10.1±0.4	8.2	13
P 6	(−529, −495)	−512	11	−18	10.0±0.4	8.1	13
P 7	(−525, −490)	−509	14	−17	12.6±0.5	10.2	16
P10	(−518, −477)	−499	18	− 4	13.5±0.5	10.9	18
P11	(−520, −495)	−507	9	−13	13.3±0.4	10.8	17
P12 (a)	(−490, −480)	−486	3	+ 5	4.1±0.3	3.3	5
P12 (b)	(−519, −499)	−508	9	−18	11.0±0.4	8.9	14
P13	(−523, −476)	−503	20	−11	20.4±0.9	16.5	27
P14	(−524, −465)	−503	23	−13	16.2±0.7	13.1	21

† The numbers were obtained by the following equations:

$$N_{H_2}=\cos i\times 3.6\times 10^{20}\int T_A^* dV(H_2\ \mathrm{cm}^{-2}),\quad \sigma_{H_2}=\cos i\times 5.8\int T_A^* dV\ (M_\odot\ \mathrm{pc}^{-2})$$

with the inclination of M31, $i=77°$ (T_A* in K, V in km s^{-1}) (Sanders et al. 1984).

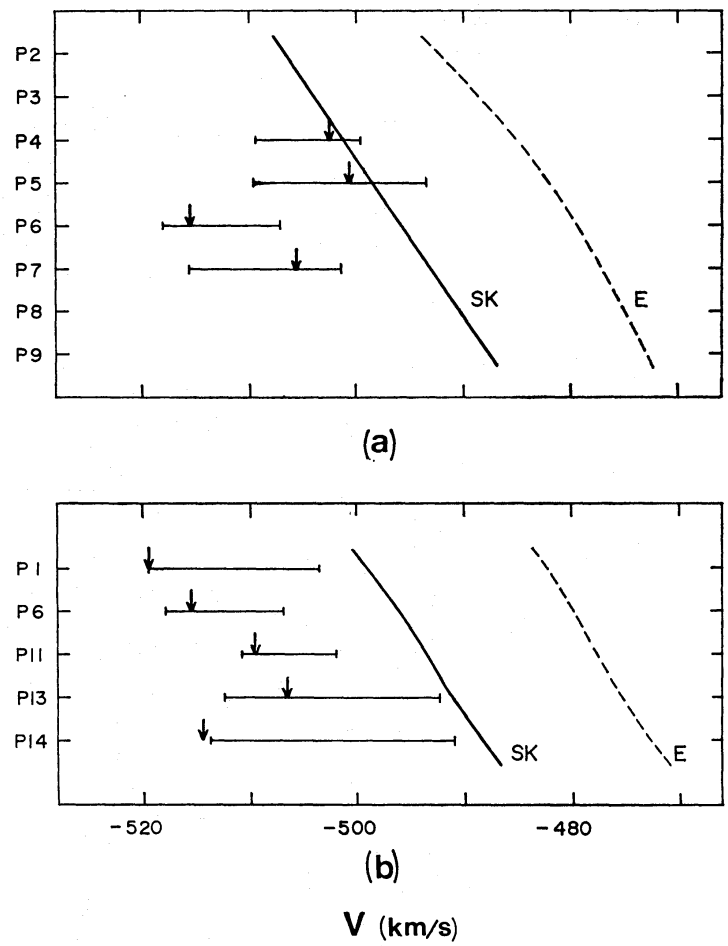

Fig. 4. Comparison of the velocities of the observed emission lines with radial velocities calculated from the rotation curves of Sofue and Kato (1981) (SK) and Emerson (1976) (E), (a) along the minor axis and (b) along the major axis. The observed velocity witdth, ΔV, is shown by a solid line for each point. Arrows indicate the positions of the mean velocity $\langle V \rangle_{CO}$ given in table 2.

We find in figure 3 several broad and narrow emission features. The derived quantities for these features are shown in table 2, where $\langle V \rangle_{CO}$ is the mean velocity (heliocentric) in the range V_1 and V_2 presented in the second column and ΔV is the full velocity width at half intensity. The antenna temperatures integrated over the same velocity ranges are listed in the sixth column. Following the empirical relation given by Sanders et al. (1984), we have deduced the face-on column density of molecular hydrogen N_{H_2}, and the face-on surface mass density σ_{H_2} for each point from the integrated intensity of the observed CO emission. These results are shown in the last two columns. We take the inclination of M31 to be $i=77°$.

In figure 4, the observed mean velocities and velocity widths are compared with the rotation curves of Emerson (1976) and Sofue and Kato (1981). The differences between the observed velocities and those expected from the circular rotation are listed in the fifth column of table 2, where V_{rot} is the heliocentric radial velocity calculated from the rotation curve of Sofue and Kato (1981) with the systemic velocity -300 km s^{-1} of M31. Figure 5 shows the velocity difference and the surface density σ_{H_2}

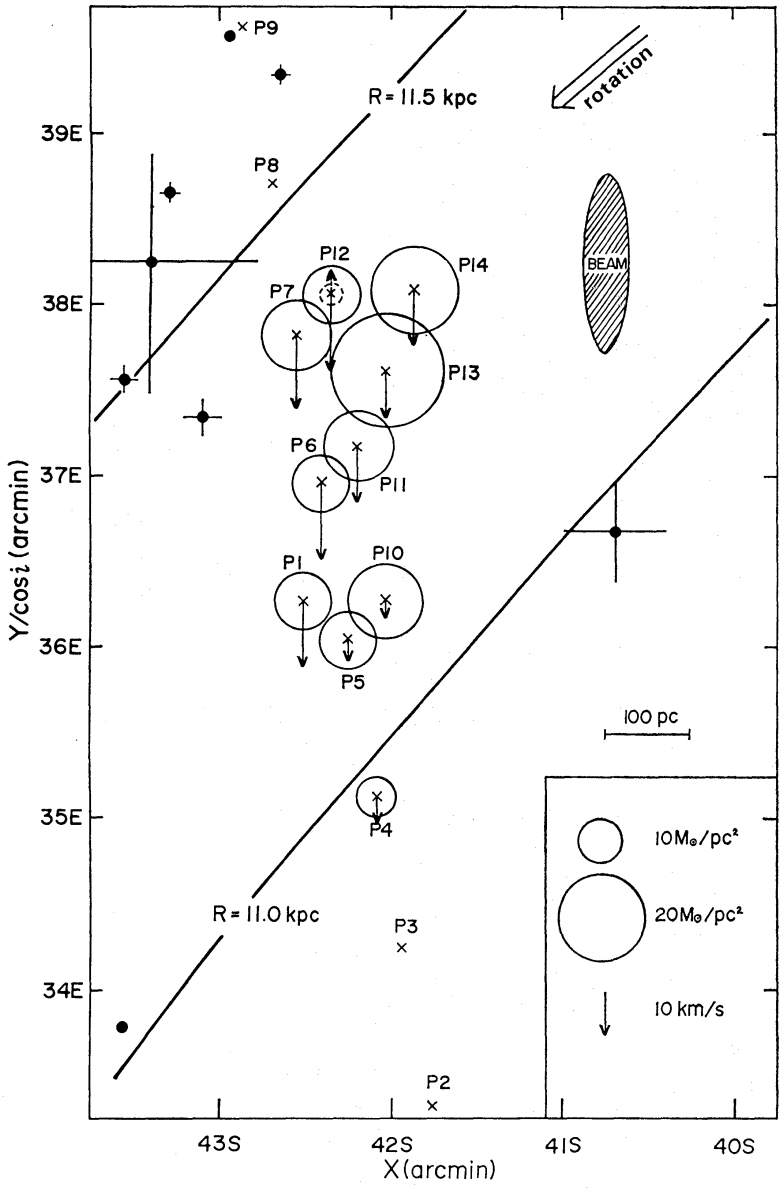

Fig. 5. The distributions of the surface density of hydrogen molecule σ_{H_2} and the velocity difference between the present observations and the rotation curve as projected onto the galactic plane of M31. Here X and Y are the directions of the major and minor axes of M31 following the coordinates of Brinks and Shane (1984). We took the inclination of M31 to be $i=77°$. Each observed point is shown by a cross with a circle, the diameter of which is proportional to σ_{H_2}. The arrows indicate the difference of the observed velocities from the circular rotation, $(\langle V\rangle_{CO}-V_{rot})/\cos i$, where downward arrows represent negative deviation and upward arrows positive deviation. Filled circles are the positions of H II regions in the catalog of Pellet et al. (1978); the bars indicate rough size of the H II regions. The solid curves show equidistance R from the center of M31.

as seen face-on. The distribution of the surface density as a function of the galactocentric distance R is presented in figure 6. To compare our result with the CO observations made by Boulanger et al. (1981), their results are also projected onto face-on

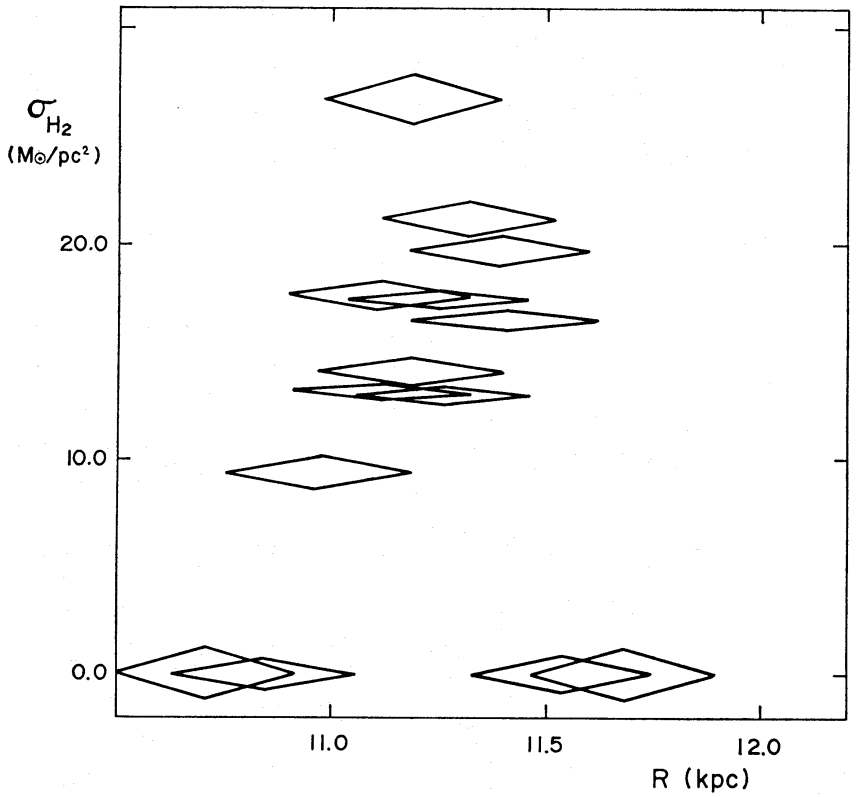

Fig. 6. The distribution of the surface density of molecular hydrogen across the arm as a function of the galactocentric distance R. The size of a diamond represents the effective beam size 400 pc in the R direction (see text) and the observational error in the integrated intensity.

position in figure 7. The positions of H II regions cataloged in Pellet et al. (1978) are presented in figures 5 and 7.

4. Conclusion and Discussion

4.a. Structure across the Arm

Figure 5 shows the distribution of the projected surface density of molecular hydrogen as seen face-on. The distribution across the arm is presented in figure 6 as a function of the galactocentric distance R. The surface luminosity of the stellar disk at the present position is nearly the same in blue to infrared wavelengths as in the solar neighborhood (de Vaucouleurs 1958; Ishida and Mikami 1982; Hiromoto et al. 1983). Assuming the same mass-to-luminosity ratio, the total surface mass densities are considered to be also nearly the same. Since the velocity dispersion of the CO clouds at the present region is observed to be as large as in the solar neighborhood (discussed later in section 4.c), we adopt 65 pc for the half width of the CO emitting region, which is comparable to the average width of our Galaxy (Sanders et al. 1984). Given that the inclination of the disk is 77°, the stratified distribution of the CO emitting region with its half width broadens the effective beam size of our observations to 600 pc in the minor-axis direction and to 400 pc in the R direction. Sawa and Sofue

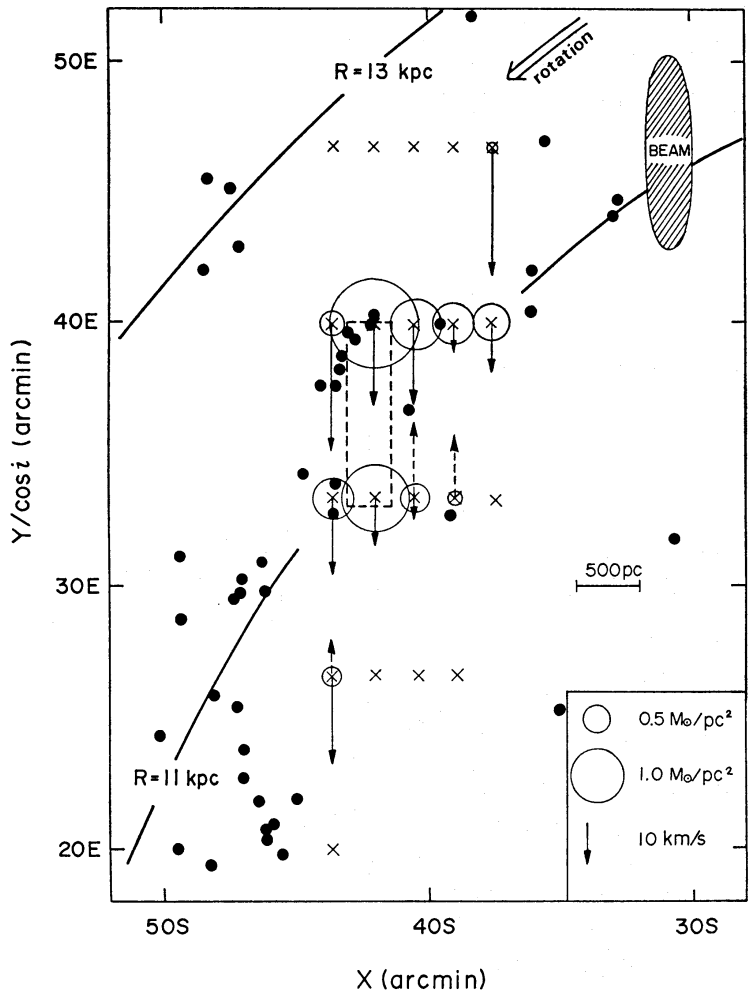

Fig. 7. The result of CO observations by Boulanger et al. (1981) with a resolution of 1′.7. Notations are the same as in figure 5. A small box with broken lines indicates our observational field.

(1982) obtained an overall picture of the warp in the whole disk of M31 through an analysis of H I-line data. According to their results, the displacement of the present position from the flat disk is less than 200 pc. The displacement will locally change the inclination to 78°.5 at most. Therefore, the warp will not seriously affect the following discussions.

It appears from figure 6 that the CO-arm width is about 500 pc or less. The apparently much larger arm width seen in Boulanger et al. (1981) is most likely due to their wider beam width of 1′.7 which corresponds to about 1.5 kpc in the R direction. We note that the CO-arm width obtained in the present observations is much narrower than the H I-arm width derived from the high-resolution observations by Brinks and Shane (1984); the H I-arm width is about 1–2 kpc in the present field.

Pellet et al. (1978) presented the distribution of H II regions in M31. A complex of H II regions is located near the edge of our investigated region (see figures 5 and 7). The observed points, P8 and P9 in the complex, have no indication of CO emission. Although further observations with more coverage in the complex should be made,

the present result suggests that the CO emitting region avoids the H II regions.

4.b. Surface Density of Hydrogen Molecule

The average integrated intensity of the CO line emission on the ten points, where the line has been detected (see table 2) is about 12.9 K km s^{-1}. This amount leads to the column density of hydrogen molecule, $N_{H_2}=4.6\times10^{21}$ H_2 cm^{-2}, or $73M_\odot$ pc^{-2}. Recalling that the inclination is 77°, we calculate the surface density of molecular hydrogen as projected on the galaxy plane to be $16M_\odot$ pc^{-2}. This value is comparable to the surface densities of nearby spiral galaxies (Solomon 1983). Although there may be error in the derived density by at least a factor 2 due to uncertainty in the assumptions of similar gas-to-dust, carbon-to-hydrogen, or ^{12}CO-to-^{13}CO ratios in the external galaxies and in our Galaxy (e.g. Encrenaz et al. 1979), it is still an order of magnitude higher than the mean surface density so far derived for M31 (Solomon 1983). However, the higher value for M31 is reasonable, because our beam has almost resolved the narrow spiral arm.

4.c. CO Clouds

We find in figure 3 broad line-width features having a velocity width of ΔV=9–23 km s^{-1} in addition to several cloudlike narrow emission features of ΔV=3–5 km s^{-1}. Velocity gradient across the beam size of 14″ due to the galactic rotation can be estimated by using the rotation curve of Sofue and Kato (1981). The gradient across the beam in the direction of the major axis is about 0.3 km s^{-1}, while it is 3 km s^{-1} in the direction of the minor axis. The contribution of the thickness of the CO emitting layer with the half width of 65 pc broadens the line width to 8 km s^{-1}. Accordingly the velocity gradient within the beam cannot account for the broad line widths observed in several points. It is also unlikely that individual CO clouds have such a internal velocity width (Larson 1981). It is therefore concluded that the broad line components in table 2 are caused by a large number of small clouds with the cloud-to-cloud velocity dispersion comparable to that in the solar neighborhood; in fact we recall that molecular clouds in the solar neighborhood typically have one dimensional r.m.s. cloud-to-cloud velocity dispersion of 5–9 km s^{-1} (Stark 1979, 1984; Sanders et al. 1984; Blitz et al. 1984), which leads to the FWHM velocity width of about ΔV=11–25 km s^{-1} as a whole.

Besides the broad emission lines, there have been detected several cloudlike emission features of ΔV=3–5 km s^{-1} with T_A^*=0.3–0.5 K, for example, (position, V_{CO})=(P6, −516 km s^{-1}) ($T_A^*=5\sigma_{rms}$), (P7, −506 km s^{-1}) ($T_A^*=4\sigma_{rms}$), and (P12, −487 km s^{-1}) ($T_A^*=7\sigma_{rms}$). Their masses are estimated as follows. If the ^{12}CO optical depth of the clouds is very large ($\tau\gg1$), as is the case in our Galaxy, the observed antenna temperature T_A^* is expressed by the following equation:

$$T_A^*\simeq T_B\eta_B f, \qquad (1)$$

where T_A^* is brightness temperature of the cloud, η_B=0.3 the main beam efficiency, and f the filling factor of the cloud in the main beam. Assuming the same brightness temperature T_B=4–8 K of the clouds as in our Galaxy (e.g. Dickman 1978; Solomon and Sanders 1980), we will observe T_A^*=0.3–0.5 K if the cloud has size of 17–30

pc in diameter and is located in the main beam of 47 pc. The cloud of such size in our Galaxy typically has a mass of $(2\text{–}6)\times10^4 M_\odot$ (Larson 1981). On the other hand, the observed velocity width ΔV=3–5 km s^{-1} of the clouds gives the virial mass of $(1\text{–}5)\times10^4 M_\odot$, which is consistent with the mass obtained above. Therefore, it is concluded that the CO emission in the arm of M31 comes from several clouds with the mass of $(2\text{–}6)\times10^4 M_\odot$ as well as many smaller clouds, if the properties of the CO clouds in M31 are similar to those in our Galaxy.

4.d. Velocity Field

The mean velocities of the CO emission features in table 2 are mostly distributed near -510 km s^{-1} (see figure 4). We find a large systematic difference of the observed CO velocities from the radial velocities expected from a circular rotation; most of the observed velocities are less than those expected from the rotation curve of Sofue and Kato (1981) by 9–18 km s^{-1}. Deceleration of the CO clouds by a spiral arm shock is suggested for such a systematic deviation. On the other hand, the points P4, P5, and P10 outside the dense arm have similar velocities to that of the circular rotation. We can naturally consider that these points are still in pregalactic shock positions, where the cloud flow obeys the mean galactic rotation.

The authors wish to express their hearty thanks to the staff members of the Nobeyama Radio Observatory. The data processing was carried out with FACOM-M200 and M180IIAD at NRO, and FACOM-M382 at the Data Processing Center of Kyoto University.

References

Blitz, L. 1981, in *Extragalactic Molecules, Proceedings of a Workshop held at the NRAO*, ed. L. Blitz and M. L. Kutner (Publications Division, NRAO, Green Bank, West Virginia), p. 93.
Blitz, L., Magnani, L., and Mundy, L. 1984, *Astrophys. J. Letters*, **282**, L9.
Boulanger, F., Stark, A. A., and Combes, F. 1981, *Astron. Astrophys.*, **93**, L1.
Brinks, E., and Shane, W. W. 1984, *Astron. Astrophys. Suppl.*, **55**, 179.
Combes, F., Encrenaz, P. J., Lucas, R., and Weliachew, L. 1977, *Astron. Astrophys.*, **61**, L7.
de Vaucouleurs, G. 1958, *Astrophys. J.*, **128**, 465.
Dickman, R. L. 1978, *Astrophys. J. Suppl.*, **37**, 407.
Emerson, D. T. 1976, *Monthly Notices Roy. Astron. Soc.*, **176**, 321.
Encrenaz, P. J., Stark, A. A., Combes, F., and Wilson, R. W. 1979, *Astron. Astrophys.*, **78**, L1.
Hiromoto, N., Maihara, T., Oda, N., and Okuda, H. 1983, *Publ. Astron. Soc. Japan*, **35**, 413.
Ishida, K., and Mikami, T. 1982, *Publ. Astron. Soc. Japan*, **34**, 89.
Larson, R. B. 1981, *Monthly Notices Roy. Astron. Soc.*, **194**, 809.
Pellet, A., Astier, N., Viale, A., Courtès, G., Maucherat, A., Monnet, G., and Simien, F. 1978, *Astron. Astrophys. Suppl.*, **31**, 439.
Sanders, D. B., Solomon, P. M., and Scoville, N. Z. 1984, *Astrophys. J.*, **276**, 182.
Sawa, T., and Sofue, Y. 1982, *Publ. Astron. Soc. Japan*, **34**, 189.
Sofue, Y., and Kato, T. 1981, *Publ. Astron. Soc. Japan*, **33**, 449.
Solomon, P. M. 1983, in *Internal Kinematics and Dynamics of Galaxies, IAU Symp. No. 100*, ed. E. Athanassoula (D. Reidel Publishing Company, Dordrecht), p. 35.
Solomon, P. M., and Sanders, D. B. 1980, in *Giant Molecular Clouds in the Galaxy*, ed. P. M. Solomon and M. G. Edmunds (Pergamon Press, Oxford)), p. 41.

Stark, A. A. 1979, Ph. D. Thesis, Princeton University.
Stark, A. A. 1984, *Astrophys. J.*, **281**, 624.
Stark, A. A. 1985, in *The Milky Way Galaxy*, *IAU Symp. No. 106*, ed. H. van Worden, R. J. Allen, and W. B. Burton, (D. Reidel Publishing Company, Dordrecht), p. 445.
Stark, A. A., and Blitz, L. 1978, *Astrophys. J. Letters*, **225**, L15.